DYRK1A modulates c-MET in pancreatic ductal adenocarcinoma to drive tumour growth

Jeroni Luna, Jacopo Boni, Miriam Cuatrecasas, Xavier Bofill-De Ros, Estela Núñez-Manchón, Meritxell Gironella, Eva C. Vaquero, Maria L. Arbones, Susana de la Luna, Cristina Fillat

Supplementary Methods

Cell treatments

For treatment with hepatocyte growth factor (HGF; 20 ng/mL; Sigma), cells were grown in FBS-free DMEM for 16 h to minimize basal c-MET activity. For inhibition of DYRK1A, cells were pre-incubated in the presence of harmine (10 μM; TCI Chemicals) for the times indicated. For c-MET half-life assessment, cells were incubated in the presence of cycloheximide (10 μg/mL; Panreac).

Lentiviral infections

For silencing experiments, the following lentivectors (derived from pLKO.1-puro) were obtained from the Sigma Mission collection: shRNA control, non-targeting vector (SHC001); shRNAs to DYRK1A: sh1-TRCN0000022999, sh2-TRCN0000199464, sh3-TRCN0000010613, and sh4-TRCN0000199188; shRNAs to DYRK1B: sh1-TRCN0000002139 and sh2-TRCN0000002141; shRNA to SPRY2: sh-TRCN0000007522. For rescue experiments, DYRK1A#sh4 was used to target the 3′-untranslated region, which does not interfere with DYRK1A ectopic expression driven from the open reading frame of DYRK1A cloned into the pWPI bicistronic lentiviral vector (Addgene #12254). Lentiviral particles were generated by cotransfection of the plasmids pCMVΔR8.91,[1] pVSV-G (Addgene #8454), and the shRNAs lentivectors, in HEK-293T cells by the calcium/phosphate method (Clontech). After 48 h, culture supernatants were filtered and applied directly to cells for infection; cells were selected with 1.5 μg/mL puromycin for 3-5 days.

Clonogenic assays and cumulative cell curves

For clonogenic assays, cells transduced with the lentivirus expressing the control shRNA, DYRK1A or DYRK1B shRNAs were plated at two different densities (500 and 1000 cells per well) in 6-well dishes. After 7-14 days, cells were fixed in 10% formalin

and stained with 0.1% crystal violet, and colonies were counted from triplicate plates. The graphs in Figure 2C, S2E, S2F and S2I show all counts; statistical analysis has been performed with the mean values of the independent experiments.

For growth curves, cells were seeded at 1×10^4 cells/cm^2 in triplicate. Cells were trypsinized and counted at the indicated time points. For growth curves in the presence of harmine, cells were processed similarly but grown in DMEM + 0.25% DMSO as vehicle or harmine (10 μM, 25 μM); media was changed every 24 h.

Migration and invasion assays

For migration assays, cells were seeded at $0.5x10^5$ cells/well density in 24-well Transwells (8 μm; Corning) using serum-free DMEM. The lower chamber was filled with DMEM 10% FBS. After 24 h, cells that migrated to the bottom layer were fixed with 4% paraformaldehyde (PFA) and stained with 4',6-diamidino-2-phenylindole (DAPI). Migrated cells were quantified from 5 random microscope fields.

For invasion assays, Transwells were coated with Matrigel (1:20 in phosphate buffered saline [PBS]; Corning) and cells were seeded at $0.5x10^5$ cells/well density. After 48 h, cells that invaded to the bottom layer were fixed, stained and quantified as for migration assays.

mRNA quantification

Total RNA was extracted with miRNeasy kit (Qiagen), and cDNA was generated using PrimeScript RT kit (Takara). PCR reactions were performed with the ViA7 Real-Time PCR system using SYBR Green I Master mix (Roche). In general, the template was denatured at 95ºC for 5 min and then subjected to 50 amplification cycles: 10 s/95ºC, 20 s/60ºC, and 20 s/72ºC. Primers used for qPCR are listed in supplementary table S1. Each sample was assayed in triplicate, and the Ct (threshold cycle) was calculated using the relative quantification of the second derivative maximum method with the Lightcycler 480 1.2 software (Roche). All qRT-PCR results from mice or human

samples were normalized to *Ubl4* (mice) or *UBL4A* or *HPRT* (human) mRNA levels, respectively. Data is represented as 2^CT.

Western blot

Cells washed in PBS were scraped and lysed with 50 mM Tris-HCl pH 6.8 buffer containing 4% sodium dodecyl sulfate (SDS) and 1% cOmplete™ Mini Protease inhibitor cocktail (Roche), 25 mM NaF, and 1 mM sodium orthovanadate. Protein samples were resolved by SDS-PAGE, transferred to Immobilon-P membranes (Millipore), blocked with 5% non-fat milk (5% bovine serum albumin [BSA] for phospho-antibodies) in 10 mM Tris-HCl pH 7.5, 100 mM NaCl (TBS), 0.1% Tween-20 (TBS-T), and incubated with primary antibodies overnight at 4ºC (see online supplementary table S2). Proteins were detected using horseradish peroxidase (HRP)-conjugated secondary antibodies and chemiluminescent HRP substrate (ECL Western Blotting Detection Reagents, Amersham) and visualized using ImageQuant LAS 4000 mini (GE Healthcare Life Sciences). Signals were quantified with the ImageJ software; for comparisons, the signals for each antibody were corrected by the signals of GAPDH, tubulin, or vinculin blotted in the same membranes.

***In vitro* kinase assays**

Cells were washed in PBS and then lysed in HEPES buffer (50 mM HEPES pH 7.4, 150 mM NaCl, 2 mM EDTA) with 1% NP-40, supplemented with a protease inhibitor cocktail (Roche, #11836170001), 30 mM sodium pyrophosphate, 25 mM NaF, and 2 mM sodium orthovanadate. Lysates were cleared by centrifugation and incubated overnight at 4ºC with protein A–conjugated magnetic beads (Dynabeads, Invitrogen) bound to 2-3 µg of anti-DYRK1A or -DYRK1B antibodies (Abcam, #ab69811 and #ab113968, respectively). Beads were washed 3× with HEPES buffer with 0.1% NP-40 and used either for *in vitro* kinase (IVK) assays or for Western blot analysis to control for the presence of the immunoprecipitated proteins. For the IVK assays,

immunocomplexes were washed in kinase buffer (25 mM HEPES pH 7.4, 5 mM $MgCl_2$, 5 mM $MnCl_2$, 0.5 mM DTT) and further incubated for 20 min at 30ºC in 20 µl of kinase buffer containing a final concentration of 50 µM ATP, [γ ^{32}P]-ATP (2.5×10^{-3} µCi/pmol), and 200 µM DYRKtide as the substrate peptide. Incorporation of ^{32}P was determined as described previously,[2] and kinase activity was normalized to the amount of DYRK proteins present in the immunocomplexes.

Immunohistochemistry

Tissues were fixed in 4% PFA for 24 h, embedded in paraffin, and sectioned at 2 µm. Sections were dewaxed, hydrated, and incubated in sodium citrate buffer (10 mM sodium citrate, 0.05% Tween-20, pH 6.0) at 95ºC for 30 min. Endogenous peroxidase was blocked with Dual Endogenous Enzyme Block (Dako) for 5 min. Sections were blocked with 10% FBS containing 1% BSA for 2 h at room temperature and incubated overnight at 4ºC with primary antibodies (see online supplementary table S2) diluted in PBS-T with 1% BSA. The reaction was developed using Dako EnVision + Dual Link System-HRP (DAB+) (Dako), and tissues were counterstained with Harris hematoxylin (Panreac). Stained sections were visualized with an Olympus IX51 inverted microscope and analysed by an expert pathologist. Tissues were scored (H-score) based on the total percentage of positive cells and the intensity of the staining (1+, 2+, 3+), where H= (%1+ x1) + (%2+ x2) + (%3+ x3). A minimum of 100 cells were evaluated in each section.

Data Analysis

We have reanalysed the microarray gene expression profile of pancreatic tumours and adjacent non-tumour tissues of an independent data set GSE62452.[3] The normalized expression of *DYRK1A* and *DYRK1B* was obtained using GEO2R (www.ncbi.nlm.nih.gov/geo/info/geo2r.html).

For analysis of expression in PDAC subtypes, we have used reported gene expression subtypes of pancreatic cancer from different studies: i) the two-group classification in classic or basal-like;[4] the three-group classification in classical, quasimesenchymal or exocrine like;[5] and the four group classification in pancreatic progenitor, squamous, aberrantly differentiated exocrine (ADEX) or immunogenic.[6] Gene expression data (FPKM-UQ) from TCGA-PDAC patients were normalized using Bioconductor RNAseq123 workflow package as described.[7] Clinical and molecular classification of the cohort of PDAC patients was obtained from Table S1 in the TCGA's publication,[8] and matched with *DYRK1A* corresponding gene expression using TCGA Patients Tumor Sample ID. The scripts used to perform the analysis are publicly available (github.com/xbdr86/TCGA-PAAD-subtypes). Correlation between DYRK1A levels and patients' overall survival was assessed using the TCGA and GSE62542 cohorts (for those cases with prognostic information), by the Kaplan-Meier method and evaluated with a log-rank (Mantel-Cox) test.

References

1. Zufferey R, Nagy D, Mandel RJ, et al. Multiply attenuated lentiviral vector achieves efficient gene delivery in vivo. *Nat Biotechnol* 1997;15:871-5.
2. Aranda S, Alvarez M, Turro S, et al. Sprouty2-mediated inhibition of fibroblast growth factor signaling is modulated by the protein kinase DYRK1A. *Mol Cell Biol* 2008;28:5899-911.
3. Yang S, He P, Wang J, et al. A novel MIF signaling pathway drives the malignant character of pancreatic cancer by targeting NR3C2. *Cancer Res* 2016;76:3838-50.
4. Moffitt RA, Marayati R, Flate EL, et al. Virtual microdissection identifies distinct tumor- and stroma-specific subtypes of pancreatic ductal adenocarcinoma. *Nat Genet* 2015;47:1168-78.
5. Collisson EA, Sadanandam A, Olson P, et al. Subtypes of pancreatic ductal adenocarcinoma and their differing responses to therapy. *Nat Med* 2011;17:500-3.
6. Bailey P, Chang DK, Nones K, et al. Genomic analyses identify molecular subtypes of pancreatic cancer. *Nature* 2016;531:47-52.
7. Law CW, Alhamdoosh M, Su S, et al. RNA-seq analysis is easy as 1-2-3 with limma, Glimma and edgeR. *F1000Res* 2016;5:1408.
8. Cancer Genome Atlas Research Network. Electronic address aadhe, Cancer Genome Atlas Research N. Integrated genomic characterization of pancreatic ductal adenocarcinoma. *Cancer Cell* 2017;32:185-203 e13.

Table S1: Primer sequences for qPCR

Gene	Forward	Reverse
DYRK1A/Dyrk1a	GCTGGACATCCAACATACCA	TCTGTTGCACACAAACTCCTG
DYRK1B	CGAGCAGTTTGAGTCCCCTT	ATCAGGCAATACCTGCGTGT
Dyrk1b	TCCAACGACAACAGAGCCTAC	TGATGTGTCTTGTGGGGCAC
EGFR	GACAGGCCACCTCGTCG	TGCGTGAGCTTGTTACTCGT
Egfr	TGCCACCTATGCCACGCCAAC	TGAGACCTCTGGCTGGCCCA
HPRT	GATATAAGCCAGACTTTGTTGGATTTG	CTTGAACTCTCATCTTAGGCTTTG
MET/Met	CTCCTCTGGGAGCTGATGAC	GGTGCCAGCATTTTAGCATT
UBL4A/Ubl4	GGCAGCTGATCTCCAAAGTCCTGG	AACGTTCGATGTCATCCAGTGTTA

Table S2: Primary antibodies for Western blot and immunohistochemistry

Antibody	Host	Dilution	Source
DYRK1A	mouse	1:5000 WB 1:800 IHQ	Abnova, clone 7D10, #H00001859-M01
DYRK1A	mouse	1:500 WB	Santa Cruz, clone RR.7, #sc-100376
DYRK1A	rabbit	1:1000 WB 1:200 IHQ	Sigma, #D1694
DYRK1B	rabbit	1:1000 WB 1:200 IHQ	Abcam, #ab113968
EGFR	rabbit	1:1000 WB 1:200 IHQ	Cell Signaling, clone D38B1, #4267
GAPDH	rabbit	1:10000 WB	Millipore, #ABS16
c-MET human	rabbit	1:500 WB 1:100 IHQ 1:100 IF	Cell Signaling, clone D1C2, #8198
c-Met mouse	mouse	1:1000 WB	Santa Cruz, clone B-2, #sc-8057
Phospho c-MET Y1003	rabbit	1:1000 WB	Cell Signaling, clone 13D11, #3135
Ki-67	mouse	1:100 IHQ	Dako, clone MIB-1, #M7240
Sprouty 2	rabbit	1:1000 WB	Sigma, #S1444
ERK2	rabbit	1:1000 WB	Santa Cruz, #sc-154
Phospho-ERK1/2 (Thr202/Tyr204)	mouse	1:1000 WB	Cell Signaling, #9106
α-Tubulin	mouse	1:10000 WB	Sigma, #T6199
Vinculin	mouse	1:10000 WB	Sigma, #V9131

WB: Western blot

IHQ: Immunohistochemisty

Supplementary Figure Legends

Supplementary Figure S1, related to Figure 1.

(A) Representative images of DYRK1B immunohistochemical staining in low- and high-grade PanIN and PDAC lesions, corresponding to the same samples shown in figure 1A (scale bar, 50 μm). Notice the predominant nuclear pattern of staining with DYRK1A (figure 1) and more cytoplasmic with DYRK1B. (B) qRT-PCR analysis of *DYRK1B* mRNA in pancreas tumour samples and adjacent non-tumour tissue of two independent sample sets (set 1, n=11; set 2, n=19 healthy samples, n=14, tumour samples; Mann-Whitney test). (C) *DYRK1B* mRNA levels by microarray analysis of pancreatic tumour samples (GSE62452; n=69; Student's *t*-test). (D-E) Boxplots of *DYRK1A* expression for TCGA samples classified using the published mRNA signatures from (D) Collisson *et al* (2011)[5] (classical, n=53; exocrine-like, n=62; quasimesenchymal, n=34), and (E) Moffitt *et al* (2015)[4] (basal-like, n=65; classical, n=84) (Student's *t*-test in pair-wise comparisons). (F) DYRK1A expression according to PDAC tumour grade in the TCGA cohort (grade 1, n=5; grade 2, n=75; grade 3, n=68; grade 4, n=1) and the GSE62452 cohort (grade 1, n=2; grade 2, n=35; grade 3, n=30; grade 4, n=1) (Mann-Whitney test in pair-wise comparisons; grade 1 was not included in the statistical analysis due to the low number of samples). (G) Kaplan-Meier survival curves of PDAC patients from the TCGA (n=174) and the GSE62452 cohorts (n=66), according to DYRK1A levels (top-low 50%) (Mantel-Cox test). **p<0.01; ns, not significant.

Supplementary Figure S2, related to Figure 2

(A) Western blot analysis of DYRK1A and DYRK1B proteins in PANC-1 and BxPC-3 cells. The lanes are from different parts of the same gel, indicated with a dash line. *, cross-reacting band. (B) Reduction of DYRK1A expression in PANC-1 cells transduced with three independent DYRK1A shRNAs (sh1, sh2, sh3); quantification of Western

blots signals expressed as percentage of the values in cells transduced with a control shRNA (n=5-10). (C) Confirmation of DYRK1B knockdown in PANC-1 cells transduced with two independent DYRK1B shRNAs. Images correspond to a representative experiment (NI= non infected; the lanes are from different parts of the same gel, indicated with a dash line.); the graph shows the quantification of Western blots signals expressed as percentage of the values in cells transduced with a control shRNA (n=6). (D) Cell proliferation assay of control and shDYRK1B PANC-1 cells with two independent shRNAs. The graph shows cell numbers relative at day 0, which was arbitrarily set as 1 (n=3; Mann-Whitney test). (E) Representative images of colony formation assays in shControl and shDYRK1B PANC-1 cells. The graph shows quantitative analysis of colony numbers (n=3-4 independent experiments, performed in triplicate; Mann-Whitney test). (F) Western blot analysis of DYRK1A and DYRK1B in PANC-1 cells transduced with the indicated shRNAs (the lanes are from different parts of the same gel, indicated with a dash line). The graph shows quantitative analysis of colony numbers in a representative experiment performed using 6 independent plates (Mann-Whitney test). (G) Confirmation of DYRK1A knockdown in BxPC-3 cells transduced with two independent DYRK1A shRNAs (sh1, sh2); two non-targeting shRNAs were used (Ctrl). (H) Cell proliferation assay of control and shDYRK1A in BxPC-3 cells. The graph shows cell numbers relative at day 0, which was arbitrarily set as 1 (n=4; Mann-Whitney test). (I) Silencing of DYRK1A in BxPC-3 cells significantly reduced colony formation. Images are from a representative experiment, and the graph shows the quantitative analysis of colony numbers (Mann-Whitney test). (J, K) Silencing of DYRK1B in PANC-1 cells significantly reduced their ability to migrate (J) and invade (K) in Trans-well assays (n=4; assays were done in parallel with those in figure 2D and E, sharing the Ctrl data; Mann-Whitney test). *$p<0.05$; **$p<0.01$; ***$p<0.001$.

Supplementary Figure S3, related to Figure 3.

(A) Western blot showing DYRK1A protein levels in control and knockdown PANC-1 cells transduced with two independent shRNAs to DYRK1A, used for the xenograft experiments in figure 3A (numbers correspond to band quantification). (B) DYRK1A and DYRK1B protein levels in PANC-1 xenografts (n=6 for DYRK1A; n=5 for DYRK1B; Mann-Whitney test). **p<0.01; ns, not significant.

Supplementary Figure S4, related to Figure 4.

(A) Immunostaining of DYRK1A and DYRK1B in the pancreas of wild-type mice, 16- and 20-week-old KPC mice (scale bar, 50 μm). Representative images show that DYRK1A accumulates in the nuclei of PanIN epithelial cells, while DYRK1B is distributed in both nucleus and cytoplasm. (B) qRT-PCR analysis of *Dyrk1a* and *Dyrk1b* mRNA in pancreas from KPC (20-weeks) mice compared to wild-type pancreas (Mann-Whitney test). *p<0.05.

Supplementary Figure S5, related to Figures 4 and 5.

(A, B) DYRK1B expression in pancreas of wild-type and *Ela-myc* mice detected by Western blot (A) and quantified relative to GAPDH levels (B) (n=6; Mann-Whitney test). (C) qRT-PCR analysis of *Dyrk1b* mRNA in *Ela-myc* (n=12) and wild-type mice (Wt, n=8; *Ela-myc*, n=13; Mann-Whitney test). (D) Representative images of hematoxylin and eosin (H&E) staining and Ki67 immunohistochemistry of pancreas of 11-weeks-old (n=3) and 16-weeks-old (n=2) *Ela-myc:Dyrk1a*$^{+/+}$ and *Ela-myc:Dyrk1a*$^{+/-}$ mice. (E) Quantification of Ki67 staining (Mann-Whitney test). (F) Western blot analysis of DYRK1A, EGFR and c-MET protein levels in pancreas from wild type, *Ela-myc:Dyrk1a*$^{+/-}$ and *Ela-myc:Dyrk1a*$^{+/+}$ mice. (G) Expression of *Egfr* mRNA in pancreas derived from wild type (n=7) *Ela-myc:Dyrk1a*$^{+/-}$ (n=8) and *Ela-myc:Dyrk1a*$^{+/+}$ (n=15) mice assessed by qRT-PCR (one-way ANOVA). *p<0.05, **p<0.01, ns, not significant.

Supplementary Figure S6, related to Figure 6.

(A, B**)** *DYRK1A* and *c-MET* (A) or *DYRK1A* and *DYRK1B* (B) mRNA levels in tumour samples in the TCGA and GSE62452 cohorts were plotted for correlation analysis (TCGA, n=181; GSE62452, n=69; Spearman's correlation test).

Supplementary Figure S7, related to Figure 7.

(A) Representative Western blot analysis of PANC-1 cells in the presence or absence of cycloheximide during the indicated times; quantification of independent experiments is shown in figure 7C. (B) DYRK1A knockdown leads to increased accumulation of DYRK1B in PANC-1 cells. Western blot analysis of DYRK1A and DYRK1B in shControl and shDYRK1A PANC-1 cells. (C) DYRK1B knockdown enhances HGF-induced c-MET degradation. Time-course of c-MET protein levels in shControl and shDYRK1B PANC-1 cells in response to HGF stimulation for the times indicated. (D) c-MET protein accumulation is reduced in BxPC-3 cells upon harmine treatment. (E) c-MET and DYRK1A protein levels in shControl and shDYRK1A BxPC-3 cells. The effect of two different shRNA sequences is shown. (F) Time course of c-MET accumulation in shControl and shDYRK1A BxPC-3 cells in response to HGF stimulation. (G) Western blot analysis of MIA PaCa-2 cells. (H) Cell proliferation assay of control and shDYRK1A MIA PaCa-2 cells. The graph shows cell numbers relative at day 0, which was arbitrarily set as 1 (n=3; not significant at any comparison, two-way ANOVA). The immunoblot confirms DYRK1A knockdown. In A, B, F, G and H, an asterisk indicates a cross-reacting band.

Supplementary Figure S8, related to Figure 8.

(A) Western blot analysis of c-MET phosphoY1003 in PANC-1 and BxPC-3 cells treated with HGF for the indicated times. Note that the BxPC-3 samples correspond to those shown in figure S7F. An asterisk indicates a cross-reacting band. (B) Western blot analysis of c-MET protein levels in HeLa cells with reduced levels of DYRK1A and

transfected with a phosphomimetic (T75D) or a non-phosphorylatable (T75A) SPRY2 variant. Quantification of c-MET is shown, relative to t=0. (C, D) DYRK1A- and DYRK1B-associated kinase activity was assessed in *in vitro* kinase assays (IVKs) using specific immunoprecipitates for each kinase. Protein levels in the immunoprecipitated samples were checked by Western blot, and autophosphorylation was determined by autoradiography (C); the kinase activity was measured using the DYRKtide peptide as a substrate (D). (E) DYRK1A- and DYRK1B-associated kinase activity was assessed in IVKs using the DYRKtide peptide as a substrate and specific immunoprecipitated samples for each kinase, which were prepared from cells stimulated with HGF for the time indicated (n=3). No statistically significant differences were observed at any time point (Mann-Whitney test).

Supplementary Figure S1
Luna *et al.*

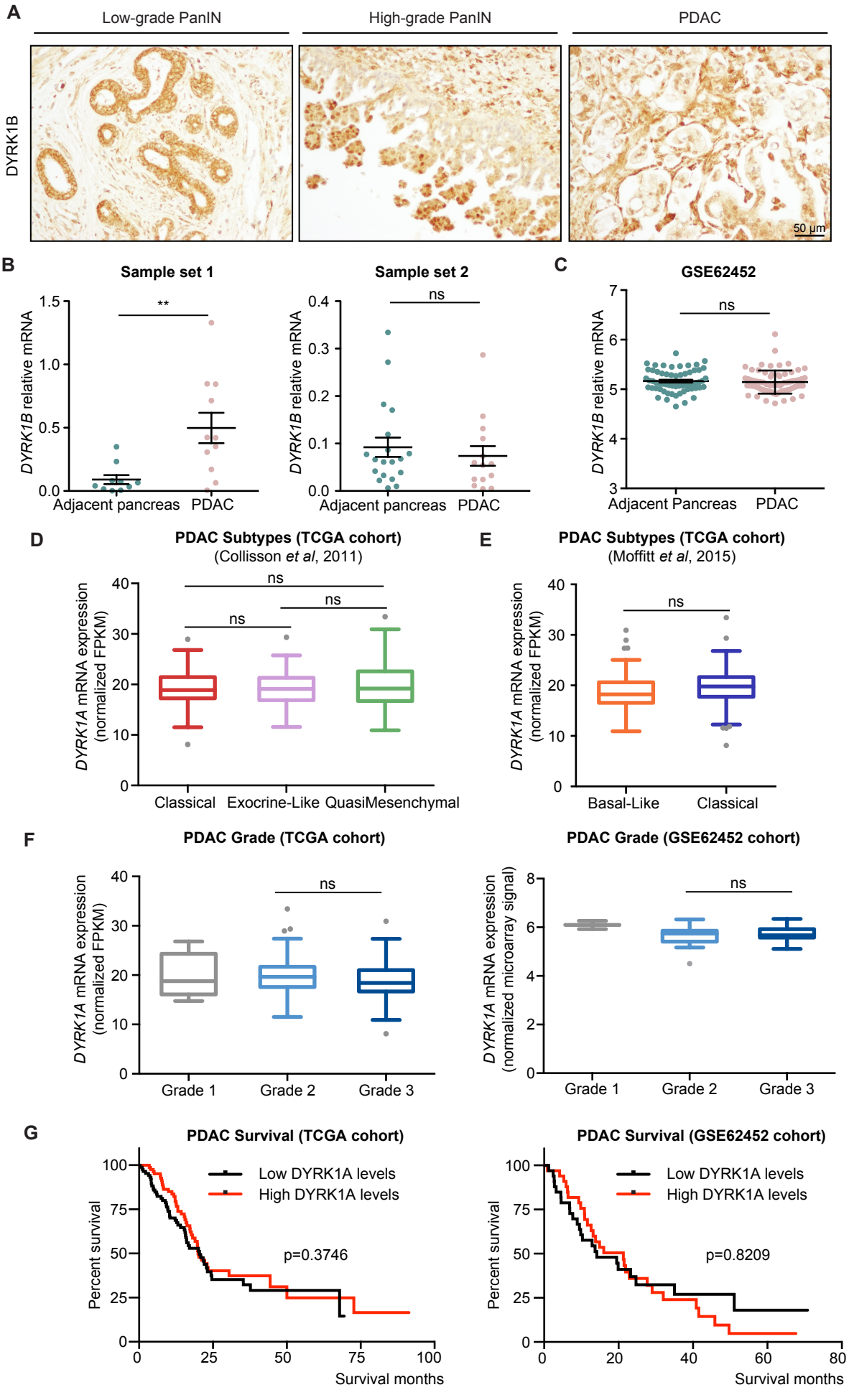

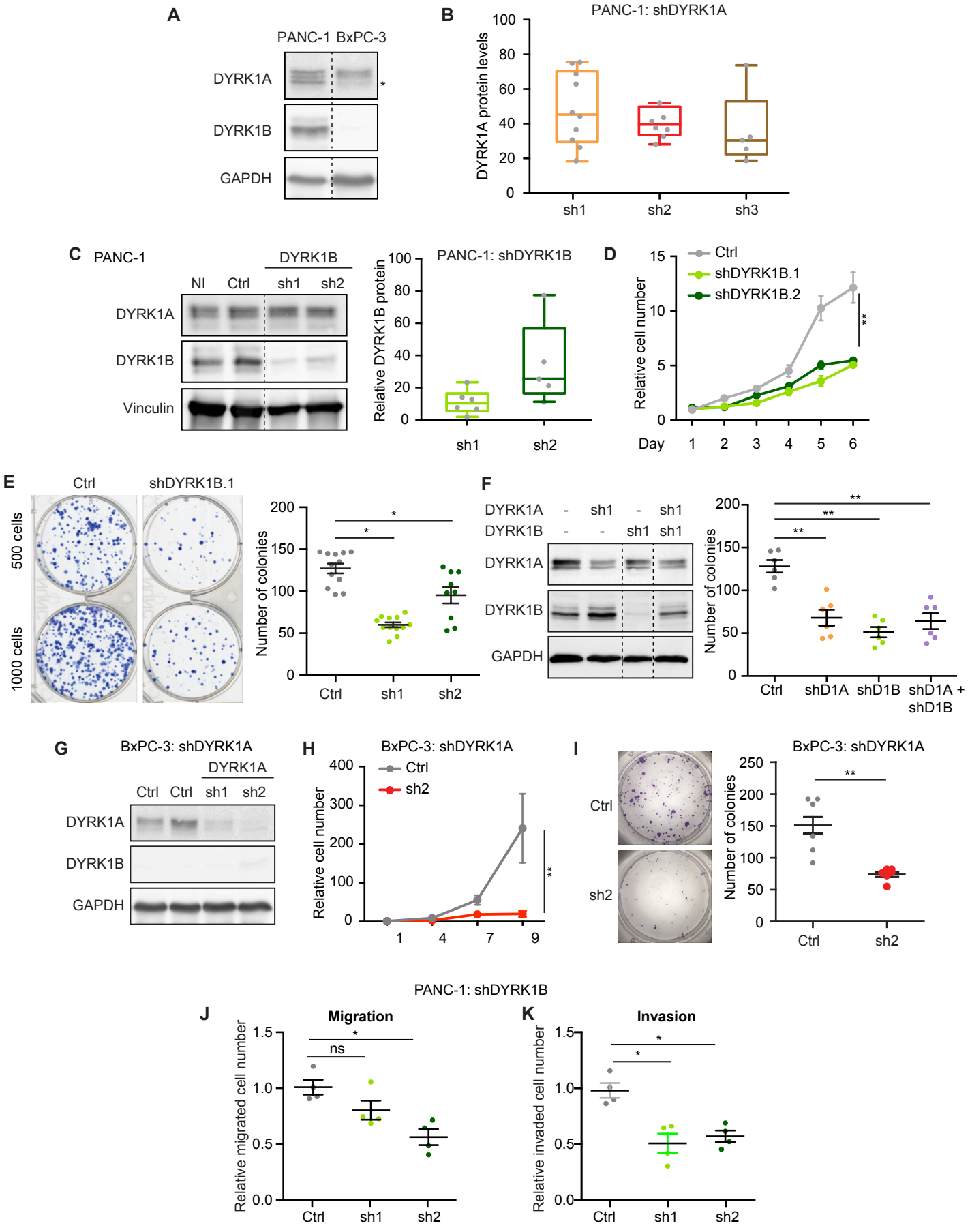
A
PANC-1 BxPC-3
DYRK1A
DYRK1B
GAPDH
B
PANC-1: shDYRK1A
DYRK1A protein levels
sh1
sh2
sh3
C
PANC-1
DYRK1B
NI Ctrl sh1 sh2
DYRK1A
DYRK1B
Vinculin
PANC-1: shDYRK1B
Relative DYRK1B protein
D
Ctrl
shDYRK1B.1
shDYRK1B.2
Relative cell number
Day
E
Ctrl
shDYRK1B.1
500 cells
1000 cells
Number of colonies
F
DYRK1A - sh1 - sh1
DYRK1B - - sh1 sh1
shD1A
shD1B
shD1A + shD1B
G
BxPC-3: shDYRK1A
DYRK1A
Ctrl Ctrl sh1 sh2
H
BxPC-3: shDYRK1A
Relative cell number
I
BxPC-3: shDYRK1A
PANC-1: shDYRK1B
J
Migration
Relative migrated cell number
ns
K
Invasion
Relative invaded cell number

Supplementary Figure S3
Luna *et al.*

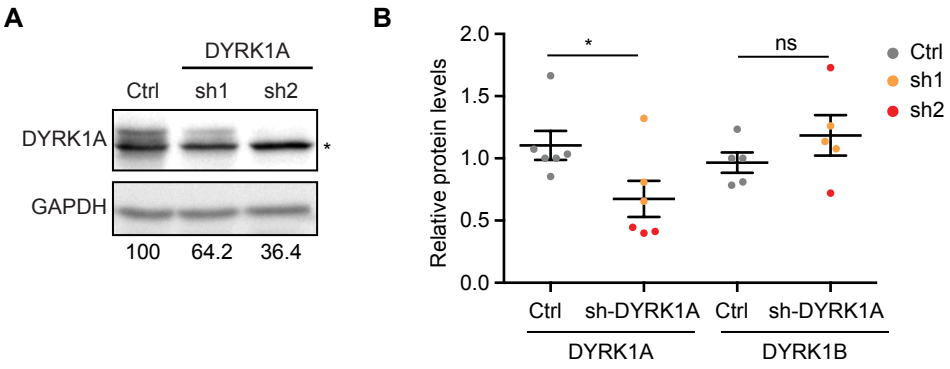

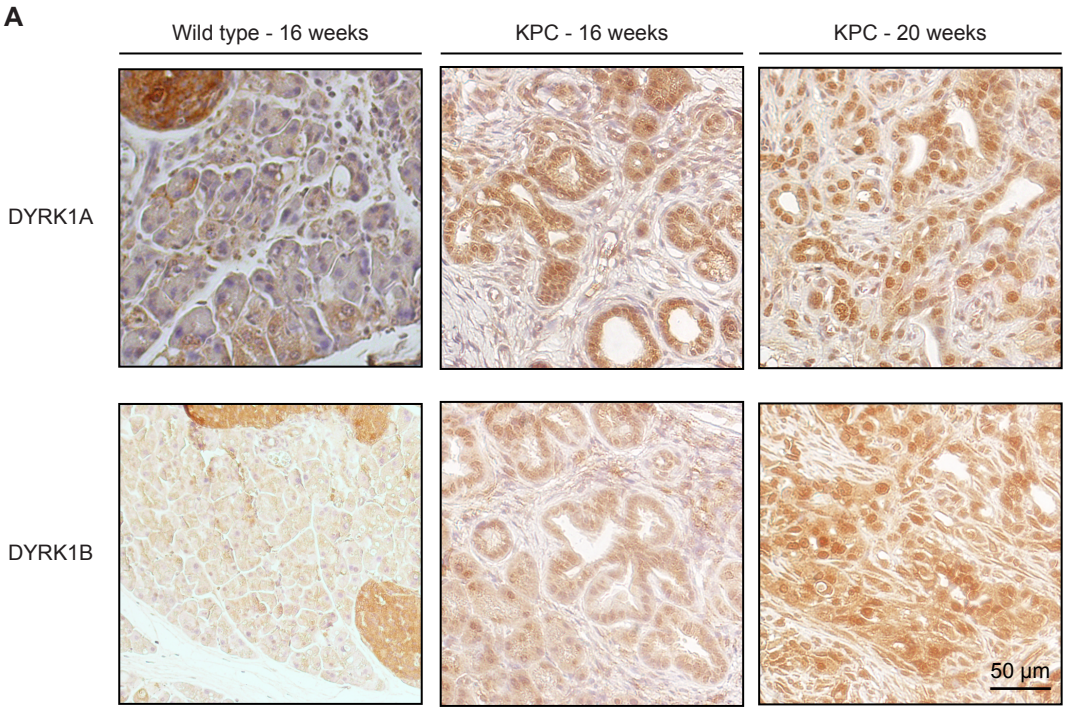
A
Wild type - 16 weeks
KPC - 16 weeks
KPC - 20 weeks
DYRK1A
DYRK1B
50 µm

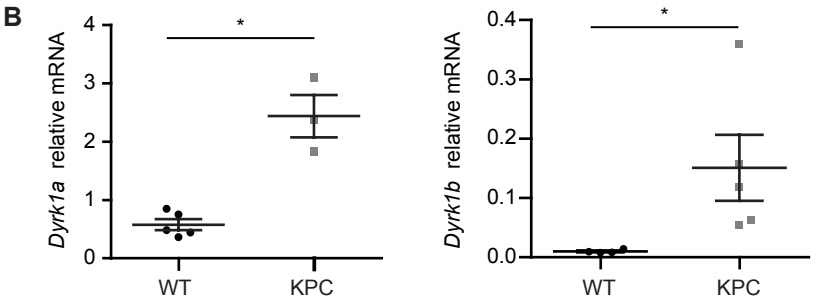
B
Dyrk1a relative mRNA
0
1
2
3
4
*
WT
KPC
Dyrk1b relative mRNA
0.0
0.1
0.2
0.3
0.4
*
WT
KPC

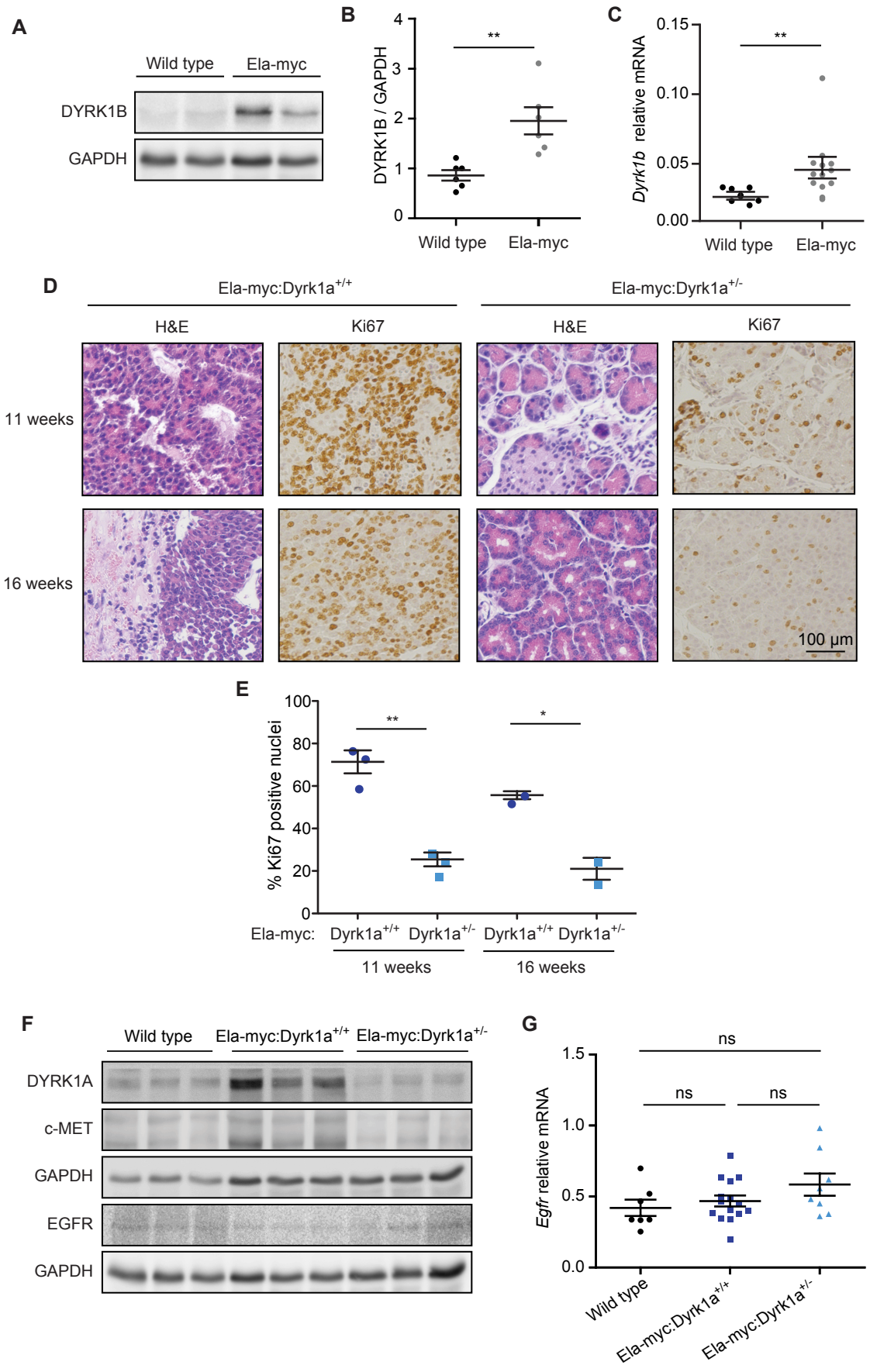
A
Wild type
Ela-myc
DYRK1B
GAPDH
B
DYRK1B / GAPDH
**
Wild type
Ela-myc
C
Dyrk1b relative mRNA
**
Wild type
Ela-myc
D
Ela-myc:Dyrk1a+/+
Ela-myc:Dyrk1a+/-
H&E
Ki67
H&E
Ki67
11 weeks
16 weeks
100 µm
E
% Ki67 positive nuclei
**
*
Ela-myc: Dyrk1a+/+ Dyrk1a+/- Dyrk1a+/+ Dyrk1a+/-
11 weeks
16 weeks
F
Wild type
Ela-myc:Dyrk1a+/+
Ela-myc:Dyrk1a+/-
DYRK1A
c-MET
GAPDH
EGFR
GAPDH
G
Egfr relative mRNA
ns
ns
ns
Wild type
Ela-myc:Dyrk1a+/+
Ela-myc:Dyrk1a+/-

Supplementary Figure S6
Luna *et al.*

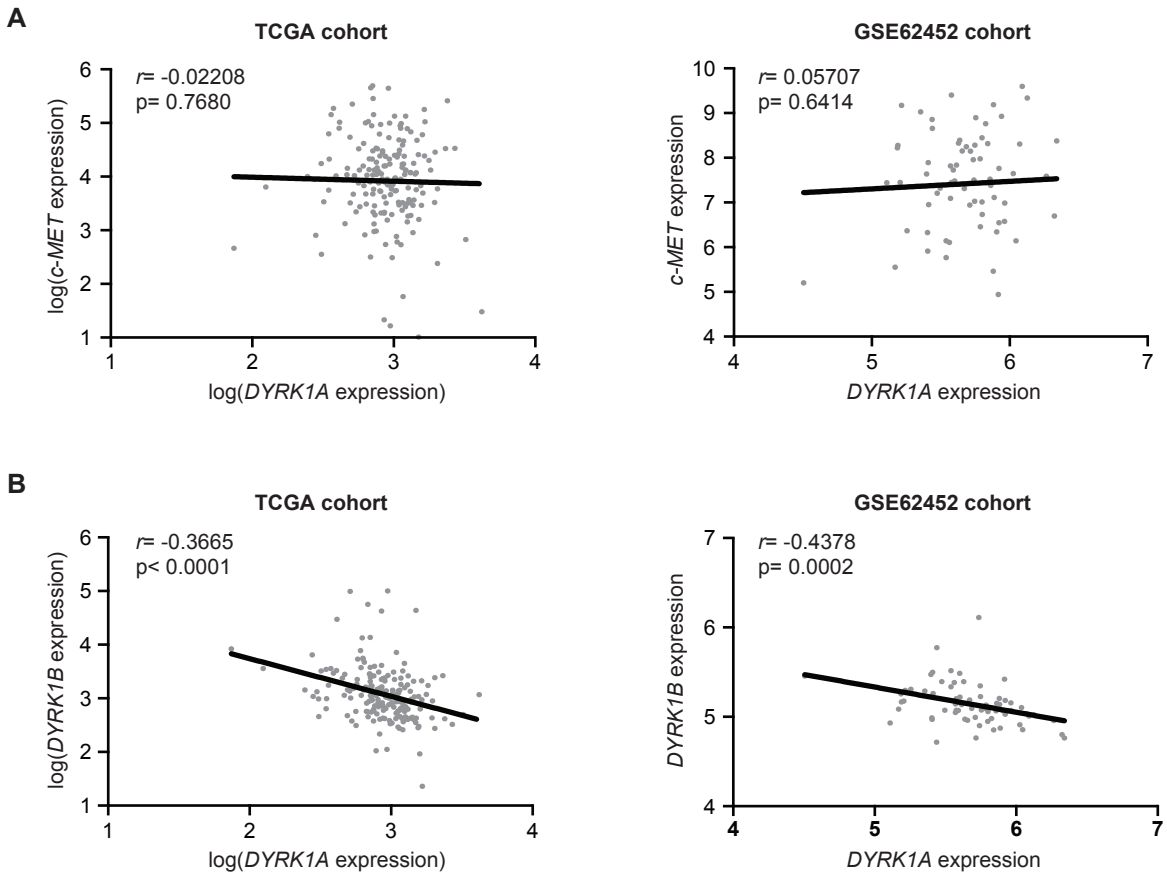

Supplementary Figure S7
Luna *et al.*

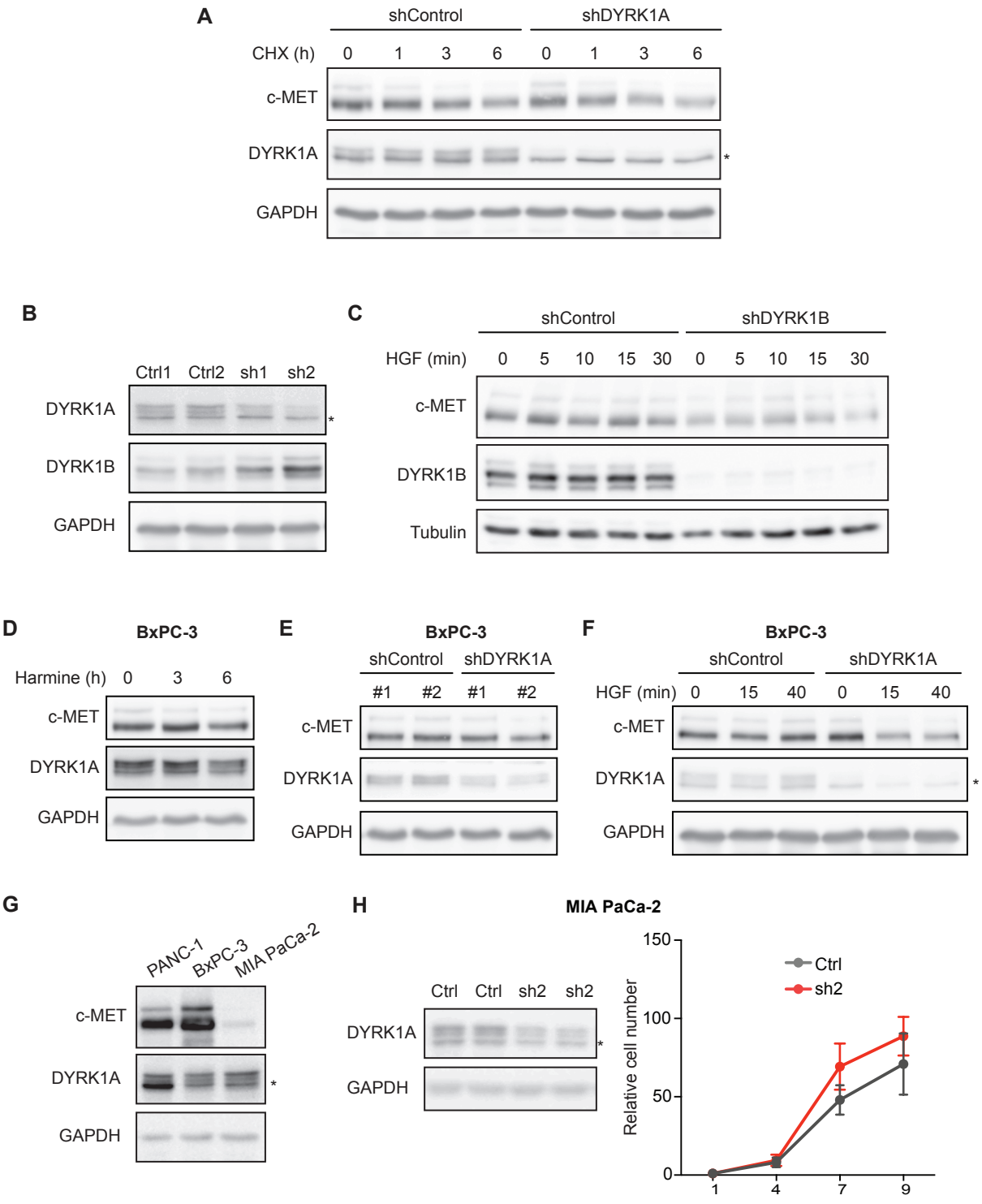

Supplementary Figure S8
Luna *et al.*